atmosphere

Article

Interdecadal Variability of Summer Extreme Rainfall Events over the Huaihe River Basin and Associated Atmospheric Circulation

Rongwei Liao [1], Ge Liu [1,2,*], Junming Chen [1,*] and Lei Zhang [3]

[1] State Key Laboratory of Severe Weather, Chinese Academy of Meteorological Sciences, Beijing 100081, China; liaorw@cma.gov.cn
[2] Collaborative Innovation Centre on Forecast and Evaluation of Meteorological Disasters, Nanjing University of Information Science and Technology, Nanjing 210044, China
[3] Tianjin Meteorological Information Centre, Tianjin 300074, China; zhanglei3505962@126.com
* Correspondence: liuge@cma.gov.cn (G.L.); chenjm@cma.gov.cn (J.C.)

Abstract: The Huaihe River basin (HRB) is an important economically developed and grain production region in China, which is severely affected by rainfall anomalies, especially extreme rainfall events (EREs). It is crucial to the features of interdecadal change in EREs and the contribution of EREs to summer-mean total rainfall amount (TRA) over the HRB. Using the observational 24-h ac-cumulated rainfall and the reanalysis products from the European Center for Medium-Range Weather Forecast (ECMWF), as well as the methods of composite analysis and Mann–Kendal and running *t* tests, we revealed that the EREs experienced a significant interdecadal increase from the period 1990–1999 to the period 2000–2009. The EREs, particularly long persistent extreme rainfall events (LPEREs), occurred more frequently over the HRB during the latter period and dominated the interdecadal increase in the summer mean TRA. An anomalous high-pressure ridge and associated anomalous anticyclone appeared around Lake Baikal during the latter period, which led to anomalous northeasterlies along the eastern flank of the anomalous anticyclone, inducing the southward intrusion of cold air flow from higher latitudes and associated anomalous ascent and more active convection over the HRB. As such, more EREs and LPEREs occurred during the latter period. The higher pseudo-equivalent temperatures also support more active convective ascent and relevant more EREs. The results may shed light on further understanding the effect of large-scale atmospheric circulation on the interdecadal variability of EREs over the HRB, helping mitigate the disastrous impacts of EREs on local ecosystems, agriculture, soil erosion, and societies.

Keywords: extreme rainfall events; interdecadal variability; Huaihe River; atmospheric circulation

check for updates

Citation: Liao, R.; Liu, G.; Chen, J.; Zhang, L. Interdecadal Variability of Summer Extreme Rainfall Events over the Huaihe River Basin and Associated Atmospheric Circulation. *Atmosphere* **2022**, *13*, 1189. https://doi.org/10.3390/atmos13081189

Academic Editors: Guocan Wu and Yuna Mao

Received: 23 June 2022
Accepted: 23 July 2022
Published: 27 July 2022

1. Introduction

The Huaihe River basin (HRB) is an important economically developed region in China and has a population of more than 178 million, accounting for 13% of the total population in China [1]. The HRB is also an important grain production area, with a cultivated land area of approximately 190 million mu, accounting for approximately 12% of the cultivated land area in China. The commodity grain production of the HRB accounts for 25% of that of China [2]. Clearly, the HRB is a key region in the food security system in China [1]. This region is located in the transition zone from subtropical to warm temperate areas [2–5] and possesses rapidly changing climate conditions, such as drought-flood abrupt alternation [6]. Hazardous climate events (e.g., extreme rainfall, floods, associated soil erosion, and landslides) often occur over the HRB, which severely affects human activities, ecosystems, agriculture, transportation, and societies [4–9], and therefore may result in catastrophic consequences [10] and severe economic losses [1]. For example, floods affected the area of 401,600 km^2 in the HRB in 1991, resulting in direct economic losses of approximately 34.0 billion RMB [1]. In 2003 (2007), the area of 259,100 (158,700) km^2 in the HRB was hit by floods, which caused economic losses of 28.6 (15.5) billion RMB [1]. In 2013, economic losses in the HRB and the Huang River basin caused by floods was up to 60 billion RMB [11]. Additionally, the HRB is an area that is experiencing severe soil erosion [12]. As reported by the Ministry of Water Resources of the People's Republic of China, in 2020 the area of soil losses in the HRB reached 20,500 km^2. A better understanding of the variability of rainfall anomalies, particularly extreme rainfall events (EREs), may improve the capabilities to mitigate the disastrous impacts of climate events on agricultural production [13], soil erosion [14,15], and the sustainable economic development [16,17]. The interdecadal variability is a main contributor to the variation in summer rainfall in eastern China [18]. Therefore, it is crucial to study whether the interdecadal variability of EREs can dominate the interdecadal variability of summer rainfall over the HRB. Furthermore, the atmospheric circulation responsible for the interdecadal variability of EREs over the HRB deserves further exploration.

Previous studies have explored the reasons for the variability in summer rainfall over the HRB on interdecadal and interannual time scales. On interdecadal time scales, some previous studies have indicated that the summer rainfall over eastern China had interdecadal shifts around the 1970s [19–21], the early 1990s [22–25], the mid-1990s [26], and the late 1990s [16,18,27]. Accompanying the interdecadal shift around the late 1990s, summer rainfall increased over the Yellow River and HRB regions and decreased to the south of the Yangtze River [18,28,29]. Different studies have emphasized that different atmospheric circulation anomalies are responsible for this interdecadal shift. For example, Zhu et al. [18] attributed the interdecadal increase in summer rainfall over the Yellow River and HRB to the strengthened ascending motion and slightly increased air humidity in situ. Huang et al. [30] also reported that summer rainfall over eastern China experienced a notable interdecadal change around the late 1990s and suggested that the weakened and poleward-shifted East Asian westerly jet played an important role in causing this interdecadal change by inducing changes in Silk Road, East Asia/Pacific, and Eurasia patterns. Zhang and Guo [31] suggested that the high-pressure anomalies around Lake Baikal, the weaker East Asian westerly jet, and anomalous circulations over the Southern Hemisphere modulated this shift and caused more (less) rainfall over the HRB (Yangtze River) during the period 2000–2007. During the period 2000–2012, the WPSH became weaker and moved eastward, which suppressed the southwesterly moisture transport, and accordingly led to more rainfall over the Yellow River and HRB regions and South China [28]. During the Hiatus period (1998–2013), the summer rainfall belt shifted from the Yangtze River to the Yellow River and HRB region, which can be attributable to the northward displacement of the East Asian westerly jet [32].

On interannual time scales, Hu et al. [33] suggested that an anomalous atmospheric circulation pattern, with anomalous high-pressure ridge over the Sea of Okhotsk and anomalous low-pressure trough over Lake Baikal, can induce the southward intrusion of cold air. Meanwhile, the west Pacific subtropical high (WPSH) is stronger and extends northward. The ridge-trough pattern and the stronger and northward-extended WPSH synergistically lead to more rainfall over the HRB, to the north of the Yangtze River [33]. Ping et al. [34] indicated that an anomalous ridge to the east of Lake Baikal and a stronger and westward-extended WPSH contribute to more rainfall over the HRB. The above studies on the interannual variability of the summer HRB rainfall showed, to some extent, discrepant results, which may be due to the different time periods focused by these studies.

The aforementioned studies primarily focused on the variability of summer mean rainfall over eastern China. Relatively few studies have investigated the variability of extreme rainfall events, especially for the interdecadal variability of extreme rainfall events over the HRB. The interdecadal abrupt of summer heavy rainfall (exceeding 50 mm day^{-1}) over eastern China occurred around the early 1990s, which is related to the stronger East Asian summer monsoon, the stronger and northward-displaced WPSH, the eastward-extended South Asian High, and the anomalous anticyclone around Mongolia [25]. This anomalous circulation pattern is different from the composite results for persistent extreme rainfall events over central and eastern China [35]. The latter revealed that both a double-blocking high type (two blocking highs near the Ural Mountains and the Sea of Okhotsk) and a single-blocking high type (a blocking high to the south of Lake Baikal) facilitate persistent extreme precipitation over the Yangtze River and the HRB [35].

The interdecadal variability of EREs over the HRB needs further study. In particular, the characteristics of the interdecadal variability of EREs may differ from that of summer mean rainfall over the HRB. Also, the background of relevant circulation anomalies causing the interdecadal variability of EREs may differ from those causing the interannual/interdecadal variability of summer mean rainfall over the HRB. The aims of the work as follows: (1) to identify when the interdecadal shift of summer EREs over the HRB occurred; (2) to indicate that the interdecadal change in EREs appear over a broad area or only individual stations in the HRB region; (3) to detect whether the interdecadal change in EREs can lead to that in summer mean rainfall over the HRB; and (4) to reveal the corresponding atmospheric circulation anomalies for the interdecadal change in EREs over the HRB and how these circulation anomalies affect the interdecadal change. This work is expected to provide further understanding of the effect of large-scale atmospheric circulation on the interdecadal variability of EREs over the HRB, which may mitigate the disastrous impacts of climate events on local ecosystems, agriculture, and societies.

2. Data and Methods

2.1. Data

In this study, we used the 24-h accumulated observational rainfall at 2419 gauge stations in China (Figure 1), which were obtained from the National Meteorological Information Centre of the China Meteorological Administration. In the HRB region (32°–35° N, 110°–121° E; see the red box in Figure 1) there are 189 stations where observational rainfall is available from June 1 to August 30 during the period 1979–2014. The daily 0.25° × 0.25° grid rainfall data generated using the method of optimal interpolation were also used in this study. The monthly atmospheric circulation data with a horizontal resolution of 0.5° × 0.5° were acquired from the European Centre for Medium-Range Weather Forecasts (ECMWF) Interim reanalysis [36,37]. The data include geopotential heights, winds, vertical speeds, relative humidity, and air temperatures, which were used to explain the link between extreme rainfall events and atmospheric circulation anomalies. The above datasets were extracted for the period from 1979 to 2014.

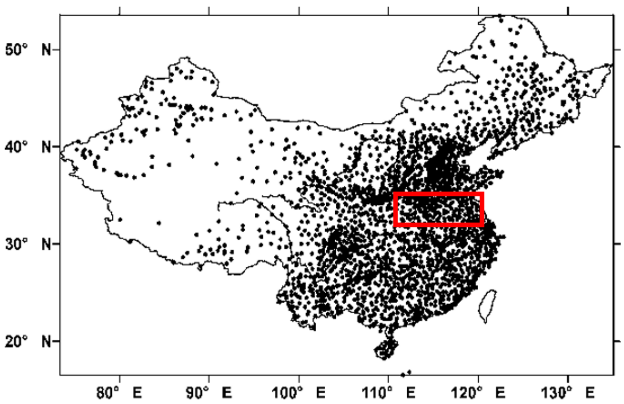

Figure 1. Spatial distribution of rain gauge stations in China, in which the red box denotes the HRB where there are 189 stations.

2.2. Methods

Extreme rainfall events (EREs) can be measured using the percentiles of precipitation [38,39]. Daily rainfall from 1 June to 31 August for each year are ranked in ascending order $(x_1, x_2, x_3, \ldots, x_n)$. The probability p that a random value is less than or equal to the rank of that value x_{my} is estimated using Equation (1) [40]. Following Bonsal et al. [40], the extreme rainfall thresholds are calculated as follows.

$$p = \frac{m - 0.31}{n + 0.38}, \tag{1}$$

$$x_{ym} = \frac{\sum_{t=1}^{y} x_{mt}}{y} \tag{2}$$

$$x_i \geq x_{ym} \tag{3}$$

where p is the 95th percentile; 0.31 and 0.38 are the empirical coefficients [38–42]; n is the number of samples ($n = 92$ days from June 1 to August 31); y is the number of years (30 years from 1981 to 2010); m is the record number within the sample size n; x_{mt} is the value of the rainfall that is specified by percentile rank p [38–40]; and x_{ym} is the 30-year mean value of x_m. Folland and Anderson [43] suggested this formula can be applied to any ranked series of continuously distributed measurements, and it is useful for an initial assessment of changing percentiles for a wide range of underlying data distributions and makes no assumptions about underlying distributions. Bonsal et al. [40] used this formula to determine the threshold of extreme temperatures in Canada. Zhai and Pan [39] used this formula to calculate the threshold of extreme rainfall over northern China. Li et al. [38] used this formula to obtain the threshold of extreme rainfall events over eastern China. The above thresholds obtained using this formula are reasonable, indicating that the formula should be suitable for many regions, including the HRB. For each station, the 95th percentile (p = 95%) of the daily rainfall distribution is estimated from June 1 to August 31 for 30 years (1981–2010). When the daily rainfall (x_i) for each station exceeds this threshold (x_{ym}), it is called an ERE.

The station-averaged total rainfall amount (TRA) is the summer mean rainfall averaged for 189 stations in the HRB. The rainfall amount (RA) contributed by the EREs over the HRB is hereafter abbreviated as RA-ERE. A long persistent rainfall event (LPRE) is defined as the rainfall over 1 mm day^{-1} persisting for 3 days or longer [16,44]. The RA contributed by the LPRE s over the HRB is abbreviated as RA-LPRE. When an extreme rainfall event occurs during a LPRE, it is called a long persistent extreme rainfall event (LPERE). Similarly, the RA contributed by the LPERE s over the HRB is abbreviated as RA-LPERE.

This study used composite analyses [45] to examine atmospheric circulation anomalies responsible for the interdecadal variability of extreme rainfall events. The Mann–Kendall and running t tests are applied to detect the abrupt change point of the interdecadal shift [16,46]. For the Mann–Kendall test, two statistics sequence curves (UF and UB) were drawn on the same figure. If there is an intersection point with the UF and UB curves falling in between the positive and negative critical lines, this intersection point is the beginning time of the interdecadal change. One can refer to the literature by Li and Sun [47] for details of the Mann–Kendall test. Statistical significance was assessed using the Student t test. All the significances are at the 90% confidence level, unless otherwise stated.

3. Results

3.1. Interdecadal Variability of EREs over the HRB

Figure 2 presents the time series of summer station-averaged RA-ERE over the HRB during the period 1979–2014, which clearly shows an interdecadal shift around the late 1990s. Furthermore, Figure 3 also show that the year of the abruptly change is 1999, that is, the interdecadal shift of the summer RA-ERE significantly occurred in 1999. The comparison between the 10-year mean RA-ERE before 1999 and that after 1999 (see the red dashed lines in Figure 2) further reveals that the JJA RA-ERE remarkably increased after 1999, with the RA-ERE during the period 2000–2009 (300 mm) significantly higher than that during the period 1990–1999 (231 mm).

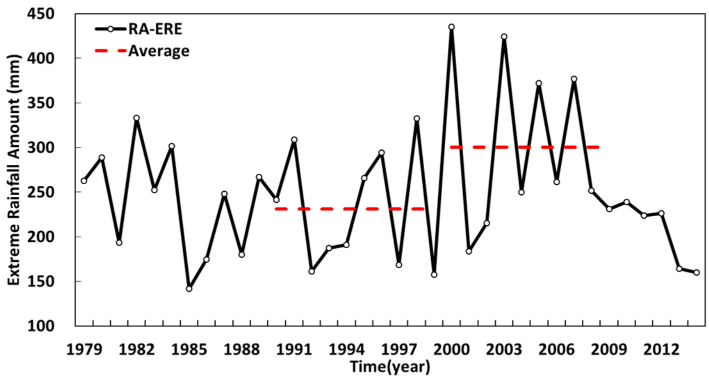

Figure 2. Time series of the summer (JJA) station-averaged rainfall amount (unit: mm) contributed by extreme rainfall events (RA-ERE, the black line with hollow circle) averaged from 189 stations over the HRB during the period 1979–2014. The two red dashed lines denote the 10-year averaged RA-ERE during the periods 1990–1999 and 2000–2009, respectively.

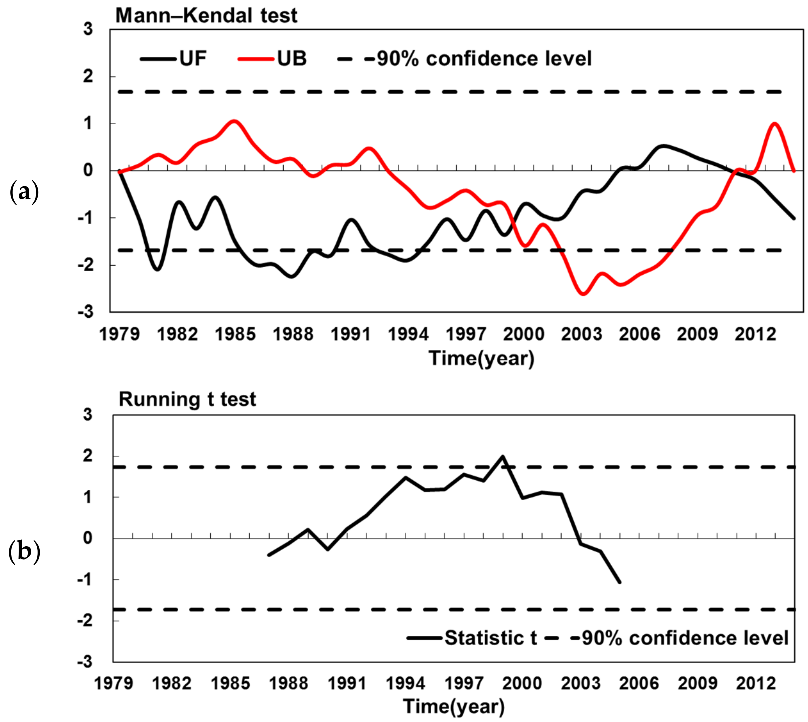

Figure 3. Mann−Kendall (**a**) and running t (**b**) tests for the time series of the summer RA−ERE over the HRB during the period 1979−2014. The two black dashed lines indicate the 90% confidence level of the two tests. In (**a**), the black line denotes the sequential statistical curve UF, and the red line denotes the re-verse statistical curve UB. The black line in (**b**) denotes the sequential statistical curve t.

Actually, the summer station-averaged TRA also experienced a significant interdecadal increase from the period 1990–1999 to the period 2000–2009. This interdecadal increase can be clearly detected in the composite difference in the summer TRA during the period 1990–1999 and that during the period 2000–2009 (Figure 4). Significantly positive anomalies appear over the HRB, with a maximum anomaly above 250 mm centered around 33° N, 115° E. Significantly negative anomalies appear over the Yangtze River basin (Figure 4). This result indicates the northward shift of summer rainfall from the Yangtze River basin to the HRB during the latter period, which is also supported by previous studies, which reported that the obvious change in summer rainfall over central and eastern China occurred in the late 1990s with an interdecadal increase in rainfall over the HRB [18,28,32,48].

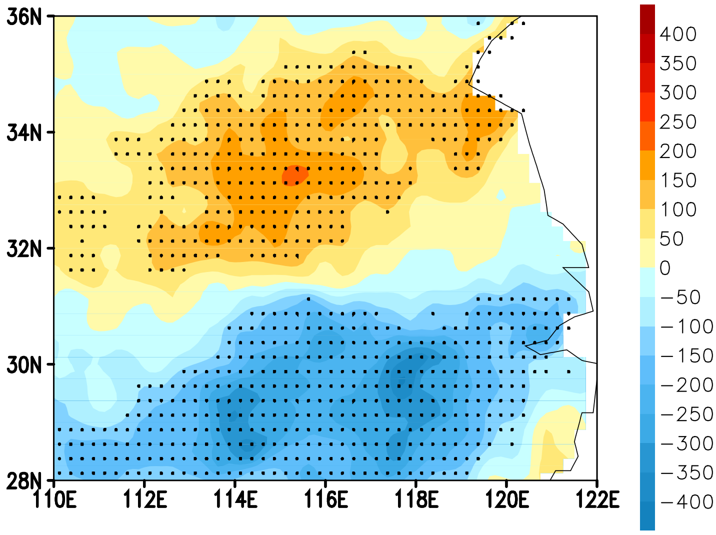

Figure 4. Composite difference of summer mean total rainfall amount (TRA; unit: mm) over eastern China between the periods 1990–1999 and 2000–2009. Significant anomalies at the 90% confidence level are stippled with black dots.

Since both the summer RA-ERE and TRA over the HRB experienced an interdecadal increase, one may wonder whether the interdecadal increase of RA-ERE can contribute most to that of TRA. Furthermore, we also compare the interdecadal changes of RA-LPRE and RA-LPERE and their contributions to the summer TRA. As shown in Table 1, from the earlier period (1990–1999) to the latter period (2000–2009), the summer TRA significantly increased by 98 mm. The summer RA-ERE significantly increased by 69 mm, accounting for 70.4% of the increase of the TRA. Also, the summer RA-LPRE (RA-LPERE) significantly increased, accounting for 71.4% (52.0%) of the increase of the TRA. The above results reveal that the EREs and LPREs play an important role in dominating the interdecadal increase of TRA over the HRB, in which the LPEREs contribute to more than half of the interdecadal increase of the TRA.

Table 1. The summer TRA, RA-ERE, RA-LPRE, and RA-LPERE over the HRB for the periods 1990–1999, 2000–2009, and the associated differences between the two periods. The superscript "*" indicates that the differences are statistically significant at the 90% confidence level.

Period (Years)	TRA (mm)	RA-ERE (mm)	RA-LPRE (mm)	RA-LPERE (mm)
1990–1999	411	231	162	100
2000–2009	507	300	232	151
difference	98 *	69 *	70 *	51 *

We further compared the number of various rainfall events between the two periods (Table 2). During the period 1990–1999 (2000–2009), the EREs appeared approximately 761 (955) times. From the earlier period to the latter one, the number of EREs significantly increased by 194. Similarly, the LPREs (LPEREs) occurred more frequently during the latter period, with the significant increases in the number of the LPREs (LPEREs) by 103 (70). Accompanying the interdecadal increase in the number of rainfall events, the number of total days when the rainfall events occurred also significantly increased (not shown).

Table 2. As in Table 1, but for the numbers of EREs, LPREs, and LPEREs, as well as the associated differences between the two periods. The superscript "*" indicates that the differences are statistically significant at the 90% confidence level.

Period (Years)	ERE	LPRE	LPERE
1990–1999	761	402	224
2000–2009	955	504	294
difference	195 *	103 *	70 *

The aforementioned results signify that from the period 1990–1999 to the period 2000–2009, the EREs, LPREs, and LPEREs over the HRB occurred more frequently and hence occupied more days in summer, resulting in, to a large extent, the interdecadal increase in the summer mean TRA over the HRB. Figure 5a presents the numbers of stations where LPREs occurred for different times during the two periods. In this figure, we can find that the number of stations where LPREs occurred for only 1–2 times clearly decreased from the earlier period to the latter period. The number of stations where LPREs occurred for three and more times increased during the latter period. The same is true for the LPEREs (Figure 5b). The above results further reveal that more frequently LPREs and LPEREs occupied more stations and larger areas over the HRB during the period 2000–2009 than during the period 1990–1999. In contrast, occasional (less than three times) rainfall events occupied fewer stations and smaller areas during the period 2000–2009. In other words, the interdecadal change of these rainfall events can be considered as a large-range phenomenon.

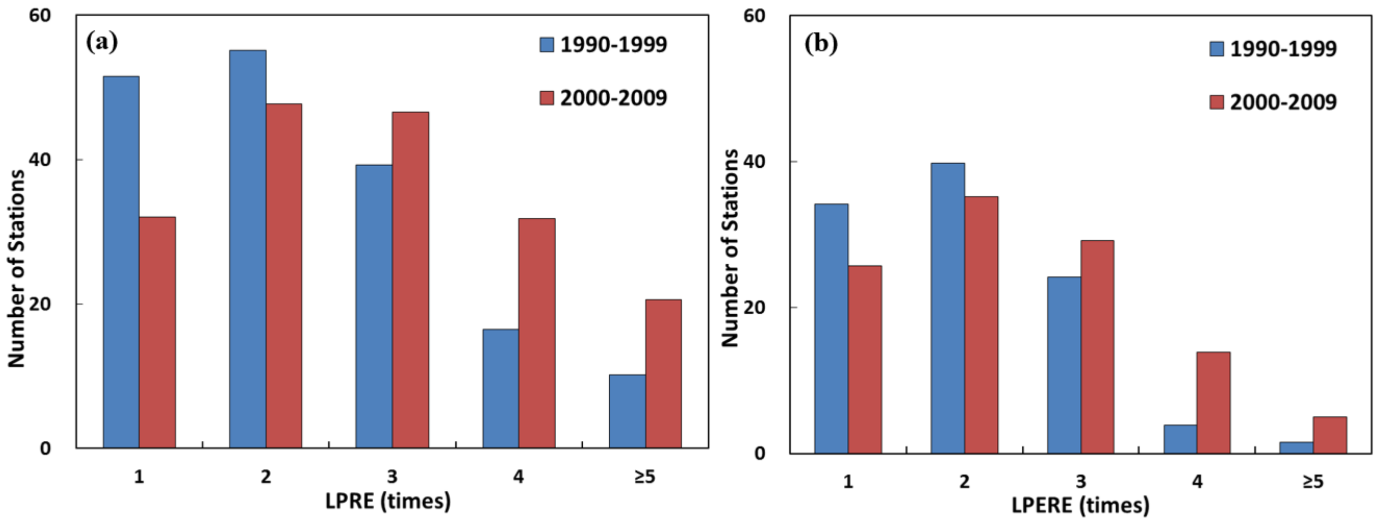

Figure 5. (**a**) The numbers of stations where LPREs occurred for different times during the two periods 1990–1999 (blue bars) and 2000–2009 (red bars). (**b**) As in (**a**), but for LPEREs.

3.2. Atmospheric Circulation Anomalies for the Interdecadal Change

Extreme rainfall events, such as heavy rainfall, are modulated by various scale systems, e.g., meso- and mircro-scale systems [49] and large-scale circulations [50]. Given that the interdecadal change of LPEREs is a large-range phenomenon over the HRB, the contribution of large-scale atmospheric circulation anomalies to this interdecadal change should be explored. Figure 6a shows the composite difference in summer 500-hPa geopotential heights between the periods 1990–1999 and 2000–2009. Significantly positive anomalies appear around Lake Baikal, with a center of exceeding 15 gpm (Figure 6a), which reflects an interdecadal increase in geopotential heights from the period 1990–1999 to the period 2000–2009. Relative to the earlier period, stronger high-pressure ridge governed Lake Baikal during the latter period (Figure 6b), inducing the southward intrusion of mid-tropospheric cold air into the HRB (Figure 7a).

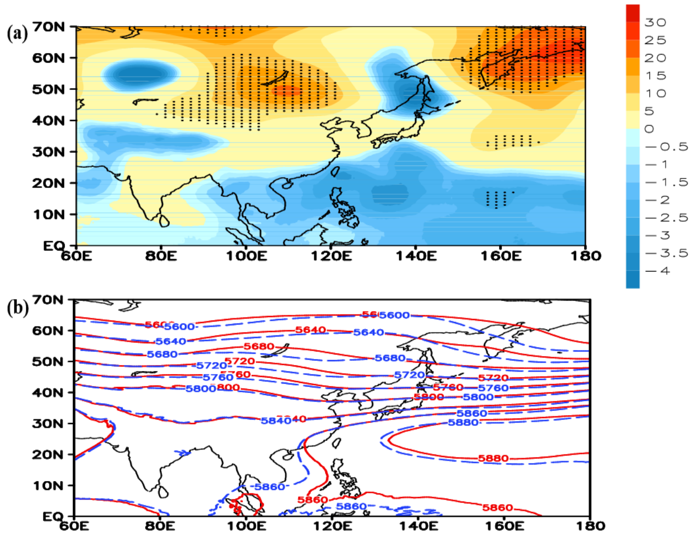

Figure 6. (**a**) Composite difference (unit: gpm) in summer 500-hPa geopotential heights between the periods 1990–1999 and 2000–2009, in which black dots denote the anomalies significant at the 90% confidence level. (**b**) Summer geopotential heights (unit: gpm) averaged for the periods 1990–1999 (blue contours) and 2000–2009 (red contours).

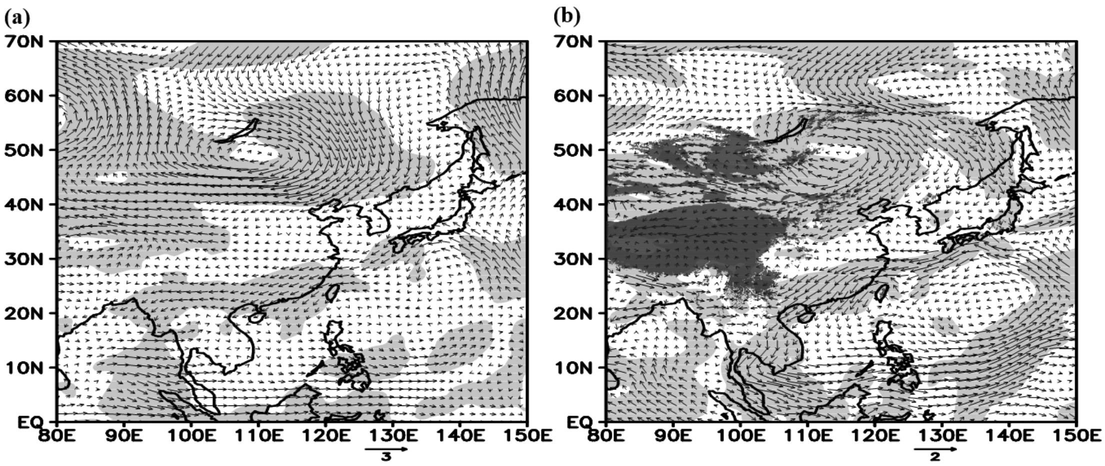

Figure 7. As in Figure 6a, but for anomalous winds (unit: $m \cdot s^{-1}$) at the 500- (**a**) and 850-hPa (**b**) levels. Shadings denote anomalous winds significant at the 90% confidence level.

Actually, significant anomalies over Lake Baikal also appeared at the upper- (200-hPa) and lower-tropospheric (850-hPa) levels (figure omitted), manifesting a quasi-barotropic structure with a thick high pressure around Lake Baikal. Corresponding to the anomalous high pressure, an anomalous anticyclone appeared around Lake Baikal and the Mongolian Plateau in the lower troposphere (Figure 7b). Along the eastern flank of the anomalous anticyclone, anomalous northeasterlies prevailed. The anomalous northeasterlies can guide the southward intrusion of the lower-tropospheric cold air from higher latitudes to the HRB and therefore facilitate more LPREs and LPEREs and associated ARA over the HRB during the period 2000–2009.

Figure 6a shows negative anomalies over the western North Pacific and the South China Sea. This reflects a weaker WPSH during the period 2000–2009 than that during the period 1990–1999, which can also be clearly detected in Figure 6b. Relative to the WPSH during the period 1990–1999 (blue 5880-gpm contour), the WPSH (red 5880-gpm contour) was relatively weaker during the period 2000–2009 (Figure 6b).

Corresponding to the weaker WPSH, an anomalous cyclone appeared over the western North Pacific and South China Sea, with anomalous northeasterlies prevailing over southern China (Figure 7a,b). Moreover, significant anomalous northeasterlies were restricted to the south of 30° N. As such, the anomalous northeasterlies can cause less water vapor transport into the Yangtze River basin and less rainfall there (Figure 4) but may not directly affect rainfall over the higher-latitude HRB.

The pseudo-equivalent temperature, which contains gravitational potential energy, internal energy, and latent heat energy, can reflect the energy in the air mass well. The composite difference of vertical pseudo-equivalent temperatures (contours in Figure 8) along 115°E between the periods 1990–1999 and 2000–2009 shows that the maximum-positive anomaly of 0.6 K appears between 700 and 600 hPa around 32°–35° N (i.e., the HRB). The pseudo-equivalent temperature anomaly above this positive center is relatively smaller. This implies that the 700–600 hPa air mass has internal energy and latent heat energy higher than the air mass with higher gravitational potential energy above it. The air mass with higher internal energy and latent heat energy tends to ascend, causing more active convective upward motions over the HRB, which can also be identified in vertical circulation anomalies over this region (vectors in Figure 8). In contrast, the negative anomalies of pseudo-equivalent temperature, which appeared to the south of the positive anomaly over the HRB, are unfavorable for convective activities over the Yangtze River Basin. Additionally, the positive and negative anomalies pseudo-equivalent temperature caused a larger gradient over the HRB (contours in Figure 8), implying that the anomalous front and associated more rainfall events appeared over this region.

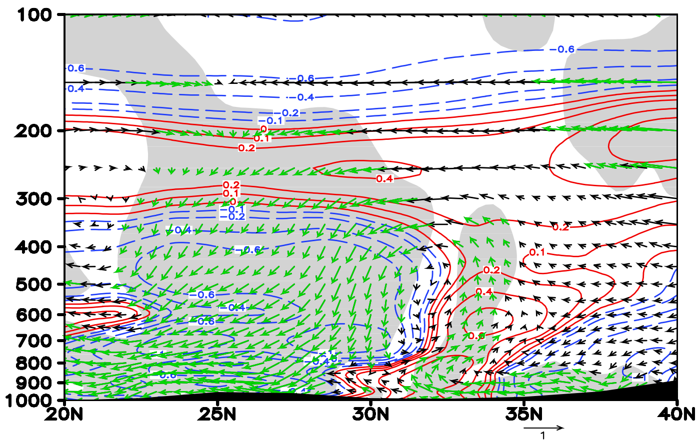

Figure 8. Composite difference of vertical circulation (vectors; unit: $m \cdot s^{-1}$ horizontal winds and $\times 0.05$ $Pa \cdot s^{-1}$ for vertical p-velocity) and pseudo-equivalent temperatures (contours; unit: K) along 115° E between the periods 1990–1999 and 2000–2009. Gray shadings denote the anomalous vertical circulation significant at the 90% confidence level (green wind vectors). Black shadings denote the terrains. Red solid contours denote the differences in pseudo-equivalent temperatures greater than or equal to 0, and blue contours denote those less than 0.

Furthermore, more active convective upward motions over the HRB may be a result from high pressure and associated anticyclonic anomalies around Lake Baikal. Specifically, this anomalous anticyclone around Lake Baikal may result in anomalous northeasterlies, inducing the southward intrusion of lower-tropospheric cold air from higher latitudes to the HRB. The composite difference of vertical circulation along 115° E between the periods 1990–1999 and 2000–2009 (vectors in Figure 8) further shows that the lower-tropospheric air flow moved southward from higher latitudes, ascended and formed an anomalous upward flow around 32°–35° N (i.e., the HRB), and turned and moved southward in the upper troposphere, and eventually descended around 25°–30° N. Clearly, the significant anomalous upward flow around 32°–35° N can promote convective activities and therefore cause more LPREs and LPEREs and associated TRA over the HRB during the period 2000–2009, while the significant anomalous downward flow around 25°–30° N may suppress convective activities and therefore lead to less rainfall over the Yangtze River Basin (Figure 4). The above result suggests that the anomalous northerly flow induced by the anomalous anticyclone around Lake Baikal can directly stimulate anomalous ascending motion over the HRB and consequently lead to more LPREs and LPEREs there.

4. Discussion

Previous studies have explored the reasons for the variability in summer mean rainfall over the HRB. Different from previous research, the present study focuses on the interdecadal variability in summer EREs over the HRB, rather than summer mean rainfall amount. The results show that RA-ERE experienced a clear interdecadal variability, with the point of change in 1999. The EREs, LPREs, and LPEREs play an important role in dominating the interdecadal increase in summer mean rainfall amount over the HRB. The above results can be considered as a supplement to previous studies on the interdecadal variability of the summer-mean rainfall amount.

Previous studies have indicated that the WPSH plays a crucial role in modulating rainfall anomalies over central-eastern China [18,28,32,48]. On interannual time scales, the stronger and westward- or northward-extended WPSH tends to enhance summer rainfall over the HRB [33,34]. However, our results reveal that for the interdecadal change in the EREs over the HRB around 1999, the WPSH did not seem to exert an important impact. Instead, the atmospheric circulation anomalies at higher latitudes, around Lake Baikal, may play a more important and more direct role. The high pressure and associated anticyclonic anomalies around Lake Baikal seem to result in anomalous northeasterlies, which guides the southward intrusion of lower-tropospheric cold air from higher latitudes to the HRB. The anomalous northeasterlies can directly promote anomalous ascending motion over the HRB and accordingly lead to more LPREs and LPEREs there. This explanation is different from previous studies on summer mean rainfall [18,30]. Previous studies [18,30] revealed a similar anomalous anticyclone around Lake Baikal, but did not attribute the anomalous ascending motion over the HRB to the anomalous anticyclone around Lake Baikal. Our detailed findings provide further explanation for the interdecadal variability in EREs over the HRB based on previous research.

5. Conclusions

In this work, we investigated the characteristics of interdecadal changes in EREs, LPREs, and LPEREs and their contribution to summer TRA over the HRB. Moreover, the associated atmospheric circulation anomalies responsible for the interdecadal changes were examined. The results show that the EREs experienced a significant interdecadal increase from the period 1990–1999 to the period 2000–2009. The EREs, in particular LPEREs, occurred more frequently during the latter period than during the earlier period. This resulted in more ERE- and LPERE-related rainfall amounts, accounting for 70.4% and 52.0% of the interdecadal increase in the summer TRA over the HRB, respectively. Moreover, the interdecadal change of these rainfall events is a large-range phenomenon over the HRB, with more frequently rainfall events occupying more stations and larger areas and occasional rainfall events occupied fewer stations and smaller areas during the period 2000–2009.

The high pressure and associated anticyclonic anomalies around Lake Baikal play an important role in causing the interdecadal increase in these extreme rainfall events and TRA. Relative to the period 1990–1999, the stronger high-pressure ridge and anticyclonic anomalies during the period 2000–2009 may lead to anomalous northeasterlies along the eastern flank of this anomalous anticyclone. The anomalous north-easterlies induced the southward intrusion of lower-tropospheric cold air from higher latitudes to the HRB. The lower-tropospheric air flow moved southward and ascended around 32°–35° N (i.e., the HRB), which contributed to more active convection and accordingly excited more EREs and LPEREs and associated TRA over the HRB during the period 2000–2009. Correspondingly, the higher pseudo-equivalent temperatures over the HRB during the latter period may also facilitate active convective upward motions and relevant rainfall events and TRA over the HRB. Moreover, the higher pseudo-equivalent temperatures over the HRB also support active convective ascent and relevant more EREs and TRA.

It should be noted that although this study emphasized the contribution of the atmospheric circulation anomalies at higher latitudes to the interdecadal change in the extreme rainfall events over the HRB, several issues remain unclear. For example, we can detect that the downward motion around 25°–30° N seems to originate from the upward motion over the HRB (Figure 8). However, it should be further explored whether the downward motion around 25°–30° N can be modulated by atmospheric circulation anomalies at lower latitudes. In addition to these atmospheric circulation anomalies, sea surface temperature anomalies in different oceans [51], ENSO [46,52], polar sea ice [53], and snow depth over the Tibetan Plateau [54,55] may affect interdecadal shifts of rainfall over eastern China. The potential physical mechanisms by which these factors influence the interdecadal change in the extreme rainfall events over the HRB through adjusting atmospheric circulation anomalies at lower latitudes deserve further investigation in the future.

Author Contributions: The study was planned and designed by R.L., and calculations were carried out and the manuscript prepared by R.L. R.L., G.L., J.C. and L.Z. have jointly modified the work. All authors discussed the results and commented on the manuscript. All authors have read and agreed to the published version of the manuscript.

Funding: This work was jointly sponsored by the National Natural Science Foundation of China (41205056), the Strategic Priority Research Program of the Chinese Academy of Sciences (XDA20100300), the Second Tibetan Plateau Scientific Expedition and Research (STEP) Program (2019QZKK0105), and the Basic Research Fund of CAMS (2021Z007).

Institutional Review Board Statement: This study was approved and guided by the Ethics Committee of the Chinese Academy of Meteorological Sciences, China Meteorological Administration.

Informed Consent Statement: Informed consent was obtained from all subjects involved in the study.

Acknowledgments: The authors acknowledge, with deep gratitude, the contribution of the anonymous reviewers whose time and effort in providing comments has improved this paper substantially.

Conflicts of Interest: The authors of this article declare that there is no conflict of interests regarding the publication of this article. The authors of the manuscript do not have a direct financial relation that might lead to a conflict of interest for any of the authors.

References

1. Qian, M.K.; Wang, K. Flood Management in China: The Huaihe River Basin as a Case Study. In *Flood Risk Management*; Hromadka, T., Rao, P., Eds.; IntechOpen: London, UK, 2017; Available online: https://www.intechopen.com/chapters/55656 (accessed on 8 July 2022). [CrossRef]
2. Guo, X.D. Regional cultural characteristics of the Huaihe River south north transition zone. *J. Bengbu Coll.* **2012**, *2*, 121–125. Available online: http://www.bbc.edu.cn/s/73/ (accessed on 8 July 2022). (In Chinese).
3. Qian, M. Speech at the 2012 Singapore International Water Week Watershed Management Forum. *Harnessing the Huaihe River.* **2012**, *8*, 5–6. Available online: http://zh.400qikan.com/wangqi/ (accessed on 7 July 2022). (In Chinese).
4. Liu, T.; Gao, X.Q.; Tan, G.R.; Fan, Y.Y.; Hui, X.Y. Statistical analysis of summer heavy rainfall events over Jianghuai region of China. *Plateau Meteorol.* **2019**, *38*, 136–142. (In Chinese) [CrossRef]
5. Fu, Y.F.; Luo, J.; Wang, D.Y.; Qiu, X.X.; Wang, S.N. A review of studies on climate change of summer precipitation in the Jianghuai region. *Torrential Rain Disasters* **2020**, *39*, 317–324. (In Chinese)
6. Xu, M.; Ding, X.J.; Luo, L.S.; Cheng, Z.; Xu, S. A possible cause of the low frequency circulation of summer-time drought-flood abrupt alternation over the Huaihe River basin. *Acta Meteorol. Sin.* **2013**, *1*, 86–95. (In Chinese) [CrossRef]
7. Rosenberg, E.A.; Keys, P.W.; Booth, D.B.; Hartley, D.; Burkey, J.; Steinemann, A.C.; Lettenmaier, D.P. Precipitation extremes and the impacts of climate change on storm water infrastructure in Washington State. *Clim. Chang.* **2010**, *102*, 319–349. [CrossRef]
8. Schoof, J.T.; Robeson, S.M. Projecting changes in regional temperature and precipitation extremes in the United States. *Weather. Clim. Extrem.* **2016**, *11*, 28–40. [CrossRef]
9. Sun, S.Y.; Guan, Z.Y.; Jin, D.C. Variation Features of Summer Regional Daily Precipitation Extreme Events in Yangtze–Huaihe Rivers Region and Their Relationships with Rossby Wave Activities. *Chin. J. Atmos. Sci.* **2022**, *46*, 15–26. (In Chinese) [CrossRef]

10. Chen, Y.; Zhai, P.M. Precursor Circulation Features for Persistent Extreme Precipitation in Central-Eastern China. *Weather Forecast.* **2014**, *29*, 226–240. [CrossRef]
11. Yuan, Y.; Yan, D.H.; Yuan, Z.; Yin, J.; Zhao, Z.N. Spatial Distribution of Precipitation in Huang-Huai-Hai River Basin between 1961 to 2016, China. *Int. J. Environ. Res. Public Health* **2019**, *16*, 3404. [CrossRef]
12. Xu, F.; Niu, J.Q. Flood disaster and strategy of control in the Huaihe drainage basin. *J. Xuchang Univ.* **2004**, *23*, 105–109. Available online: http://xcsz.cbpt.cnki.net/WKG/WebPublication/wkTextContent.aspx?colType=4&yt=2004&tp=gklb (accessed on 20 June 2022). (In Chinese)
13. Rodrigo-Comino, J.; Senciales-González, M.J.; Yu, Y.; Salvati, L.; Giménez-Morera, A.; Cerdà, A. Long-term changes in rainfed olive production, rainfall and farmer's income in Bailén (Jaén, Spain). *EMJEI.* **2021**, *6*, 58. [CrossRef]
14. Martínez-Casasnovas, J.A.; Ramos, M.C.; Ribes-Dasi, M. Soil erosion caused by extreme rainfall events: Mapping and quantification in agricultural plots from very detailed digital elevation models. *Geoderma* **2002**, *105*, 125–140. [CrossRef]
15. Piacentini, T.; Galli, A.; Marsala, V.; Miccadei, E. Analysis of soil erosion induced by heavy rainfall: A case study from the NE Abruzzo Hills Area in central Italy. *Water* **2018**, *10*, 1314. [CrossRef]
16. Yan, P.W.; Huang, D.Q.; Zhu, J.; Kuang, X.Y.; Huang, Y. The decadal shift of the long persistent rainfall over the northern part of China and the associated ocean conditions. *Int. J. Climatol.* **2019**, *39*, 3043–3056. [CrossRef]
17. Zhao, P.; Zhu, Y.N.; Zhang, Q. A summer weather index in the East Asian pressure field and associated atmospheric circulation and rainfall. *Int. J. Climatol.* **2012**, *32*, 375–386. [CrossRef]
18. Zhu, Y.L.; Wang, H.J.; Zhou, W.; Ma, J.H. Recent changes in the summer precipitation pattern in East China and the background circulation. *Clim. Dyn.* **2011**, *36*, 1463–1473. [CrossRef]
19. Wang, H.J. The weakening of the Asian monsoon circulation after the end of 1970s. *Adv. Atmos. Sci.* **2001**, *18*, 376–386. [CrossRef]
20. Mantua, N.J.; Hare, S.R. The Pacific decadal oscillation. *J. Oceanogr.* **2002**, *58*, 35–44. [CrossRef]
21. Ding, Y.H.; Sun, Y.; Wang, Z.Y.; Zhu, Y.X.; Song, Y.F. Inter-decadal variation of the summer precipitation in China and its association with decreasing Part II: Possible causes. *Int. J. Climatol.* **2009**, *29*, 1926–1944. [CrossRef]
22. Zhou, L.T.; Huang, R.H. Interdecadal variability of summer rainfall in northwest China and its possible causes. *Int. J. Climatol.* **2009**, *30*, 549–557. [CrossRef]
23. Huang, R.H.; Chen, J.L.; Liu, Y. Interdecadal variation of the leading modes of summertime precipitation anomalies over eastern China and its association with water vapor transport over East Asia. *Chin. J. Atmos. Sci.* **2011**, *35*, 589–606. (In Chinese) [CrossRef]
24. Li, X.Z.; Wen, Z.P.; Zhou, W.; Wang, D.X. Atmospheric water vapor transport associated with two decadal rainfall shits over east China. *J. Meteorol. Soc. Jpn. Ser. II* **2012**, *90*, 587–602. [CrossRef]
25. Chen, D.; Chen, J.L.; Huang, R.H.; Liu, Y. Interdecadal changes of summertime heavy rainfall in eastern China and their large-scale circulation backgrounds. *Chin. J. Atmos. Sci.* **2016**, *40*, 581–590. (In Chinese)
26. Kwon, M.H.; Jhun, J.G.; Ha, K.J. Decadal change in East Asian summer monsoon circulation in the mid-1990s. *Geophys. Res. Lett.* **2007**, *34*, 1–6. [CrossRef]
27. Gao, T.; Wang, H.J.; Zhou, T.J. Changes of extreme precipitation and nonlinear influence of climate variables over monsoon region in China. *Atmos. Res.* **2017**, *197*, 379–389. [CrossRef]
28. Wang, L.; Qian, Y.; Zhang, Y.C.; Zhao, C.; Leung, L.R.; Huang, A.N.; Xiao, C.L. Observed variability of summer precipitation pattern and extreme events in East China associated with variations of the East Asian summer monsoon. *Int. J. Climatol.* **2016**, *36*, 2942–2957. [CrossRef]
29. Wang, H.; Li, D.L. Impacts of decadal variability in sensible heat over the Tibetan Plateau on decadal transition of summer precipitation over dominant regions of monsoon rainfall band in eastern China since the early 2000s. *Chin. J. Geophys.* **2020**, *3*, 412–426. [CrossRef]
30. Huang, R.H.; Liu, Y.; Feng, T. Interdecadal change of summer precipitation over Eastern China around the late-1990s and associated circulation anomalies, internal dynamical causes. *Chin. Sci. Bull.* **2013**, *58*, 1339–1349. [CrossRef]
31. Zhang, Q.Y.; Guo, H. Circulation differences in anomalous rainfall over the Yangtze River and Huaihe River valleys in summer. *Chin. J. Atmos. Sci.* **2014**, *38*, 656–669. (In Chinese) [CrossRef]
32. Qiu, S.; Zhou, W. Variation in Summer Rainfall over the Yangtze River Region during Warming and Hiatus Periods. *Atmosphere* **2019**, *10*, 173. [CrossRef]
33. Hu, Y.M.; Ding, Y.H.; Liao, F. A classification of the precipitation patterns during the Yangtze-Huaihe meiyu period for the recent 52 years. *Acta Meteorol. Sin.* **2010**, *68*, 235–247. [CrossRef]
34. Ping, F.; Tang, X.B.; Gao, S.T.; Luo, Z.X. A Comparative Study of the Atmospheric circulations Associated with Rainy-season Floods between the Yangtze and Huaihe River Basins. *Sci. China Earth Sci.* **2014**, *44*, 766–782. [CrossRef]
35. Chen, Y.; Zhai, P.M. Two types of typical circulation pattern for persistent extreme precipitation in Central–Eastern China. *Q.J.R. Meteorol. Soc.* **2014**, *140*, 1467–1478. [CrossRef]
36. Gibson, J.K.; Kallberg, P.W.; Uppala, S.; Hernandez, A.; Nomura, A.; Serrano, E. ERA description. *ECMWF Re-Anal. Proj. Rep. Ser.* **1997**, *1*, 72. Available online: https://www.ecmwf.int/sites/default/files/elibrary/1997/9584-era-description.pdf (accessed on 19 May 2018).
37. Dee, D.P.; Uppala, S.M.; Simmons, A.J.; Berrisford, P.; Poli, P.; Kobayashi, S.; Andrae, U.; Balmaseda, M.A.; Balsamo, G.; Bauer, P.; et al. The ERA Interim reanalysis: Configuration and performance of the data assimilation system. *Q. J. Roy. Meteor. Soc.* **2011**, *137*, 553–597. [CrossRef]

38. Li, H.M.; Zhou, T.J.; Yu, R.C. Analysis of July-August daily precipitation characteristics variation in eastern China during 1958–2000. *Chin. J. Atmos. Sci.* **2008**, *32*, 360–370. (In Chinese)
39. Zhai, P.M.; Pan, X.H. Change in extreme temperature and precipitation over Northern China during the second half of the 20th century. *Acta. Geogr. Sin.* **2003**, *58*, 1–10. (In Chinese)
40. Bonsal, B.R.; Zhang, X.; Vincent, L.A.; Hogg, W.D. Characteristics of daily and extreme temperatures over Canada. *J. Clim.* **2001**, *14*, 1959–1976. [CrossRef]
41. Jenkinson, A.F. The analysis of meteorological and other geophysical extremes. In *Synoptic Climatology Branch Memo*; 58, the U.K. Met. Office; Berkshire: Bracknell, UK, 1977; p. 41.
42. Liao, R.W.; Zhao, P.; Liu, H.Y.; Fang, X.Y.; Yu, F.; Cao, Y.J.; Zhang, D.B.; Song, L.L. A Fast Quality Control of 0.5 Hz Temperature Data in China. *Front. Earth. Sci.* **2022**, *10*, 844722. [CrossRef]
43. Folland, C.; Anderson, C. Estimating changing extremes using empirical ranking methods. *J. Clim.* **2002**, *15*, 2954–2960. [CrossRef]
44. Chen, Y.; Zhai, P.M. Persistent extreme precipitation events in China during 1951–2010. *Clim. Res.* **2013**, *57*, 143–155. [CrossRef]
45. Chen, J.M.; Zhao, P.; Yang, S.; Liu, G.; Zhou, X.J. Simulation and dynamical prediction of the summer Asian-Pacific Oscillation and associated climate anomalies by the NCEP CFSv2. *J. Clim.* **2013**, *26*, 3644–3656. [CrossRef]
46. Zhu, J.; Huang, D.Q.; Zhang, Y.C.; Huang, A.N.; Kuang, X.Y.; Huang, Y. Decadal changes of Meiyu rainfall around 1991 and its relationship with two types of ENSO. *J. Geophys. Res. Atmos.* **2013**, *118*, 9766–9777. [CrossRef]
47. Li, Z.; Sun, D.Y. Trend and Abrupt Analysis of Rainfall Change During Last 50 Years in the WeiHe Basin. *Earth Sci.* **2015**, *4*, 228–234. [CrossRef]
48. Si, D.; Ding, Y.H.; Liu, Y.J. The decadal northward shift of Meiyu rain belt in China and its causes. *Sci. Bull.* **2010**, *55*, 68–73. (In Chinese) [CrossRef]
49. Gao, S.T.; Zhao, S.X.; Zhou, X.P.; Sun, S.Q.; Tao, S.Y. Progress of research on sub-synoptic scale and mesoscale torrential rain systems. *Chin. J. Atmos. Sci.* **2003**, *27*, 618–627. [CrossRef]
50. Zhang, Q.Y.; Tao, S.Y.; Zhang, S.L. The persistent heavy rainfall over the Yangtze River valley and its associations with the circulations over East Asian during summer. *Chin. J. Atmos. Sci.* **2003**, *27*, 1018–1030. [CrossRef]
51. Xu, Z.; Fan, K.; Wang, H. Decadal variation of summer precipitation over China and associated atmospheric circulation after the late 1990s. *J. Clim.* **2015**, *28*, 4086–4106. [CrossRef]
52. Lin, Z.; Lu, R. The ENSO's effect on eastern China rainfall in the following early summer. *Adv. Atmos. Sci.* **2009**, *26*, 333–342. [CrossRef]
53. Si, D.; Zhao, P.; Wang, M.H. Inter-decadal change of the middle-upper tropospheric land–sea thermal contrast in the late 1990s and the associated Northern Hemisphere hydroclimate. *Int. J. Climatol.* **2019**, *39*, 3271–3281. [CrossRef]
54. Zhao, P.; Yang, S.; Yu, R.C. Long-term changes in rainfall over eastern China and large-scale atmospheric circulation associated with recent global warming. *J. Clim.* **2010**, *23*, 1544–1562. [CrossRef]
55. Fan, K.; Xu, Z.Q.; Tian, B.Q. Has the intensity of the interannual variability in summer rainfall over South China remarkably increased? *Meteorol. Atmos. Phys.* **2014**, *124*, 23–32. [CrossRef]